Journal of Coordination Chemistry

ISSN: 0095-8972 (Print) 1029-0389 (Online) Journal homepage: http://www.tandfonline.com/loi/gcoo20

DNA cleavage activities of two dinuclear copper coordination polymers

Q.R. Cheng, F.Q. Zhang, H. Zhou, Z.Q. Pan & G.Y. Liao

To cite this article: Q.R. Cheng, F.Q. Zhang, H. Zhou, Z.Q. Pan & G.Y. Liao (2015) DNA cleavage activities of two dinuclear copper coordination polymers, Journal of Coordination Chemistry, 68:11, 1997-2005, DOI: 10.1080/00958972.2015.1032272

To link to this article: http://dx.doi.org/10.1080/00958972.2015.1032272

Journal of Coordination Chemistry, 2015
Vol. 68, No. 11, 1997–2005, http://dx.doi.org/10.1080/00958972.2015.1032272

DNA cleavage activities of two dinuclear copper coordination polymers

Q.R. CHENG†‡, F.Q. ZHANG†, H. ZHOU†, Z.Q. PAN*† and G.Y. LIAO‡

†School of Chemistry and Environmental Engineering, Wuhan Institute of Technology, Wuhan, PR China
‡School of Materials Science and Chemical Engineering, China University of Geosciences, Wuhan, PR China

(*Received 21 October 2014; accepted 23 February 2015*)

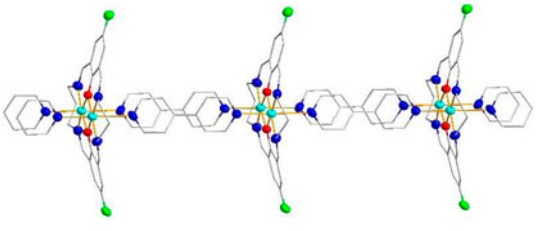

The DNA cleavage activities of two new coordination polymers of Robson-type macrocycles, $\{[Cu_2L^1(bipy)]\cdot(ClO_4)_2\cdot CH_3CN\}_\infty$ (**1**) and $\{[Cu_2L^2(bipy)]\cdot(ClO_4)_2\cdot H_2O\}_\infty$ (**2**), have been studied. The interactions of the complexes with calf thymus-DNA were studied by UV–vis and CD spectroscopic techniques. The complexes exhibit good DNA cleavage activity. The results show that the substituent on the benzene ring plays an important role in DNA cleavage and the cleavage process occurs via oxidative cleavage.

The DNA cleavage activities of two coordination polymers of Robson-type macrocycles, $\{[Cu_4L^1(4,4'\text{-bipy})_2](ClO_4)_4\cdot H_2O\}_\infty$ (**1**) and $\{[Cu_4L^2(4,4'\text{-bipy})_4](ClO_4)_4\cdot 2CH_3CN\cdot 2H_2O\}_\infty$ (**2**) (where H_2L^1 and H_2L^2 are the [2 + 2] condensation products of 1,3-diaminopropane with 2,6-diformyl-4-methylphenol and 2,6-diformyl-4-fluorophenol, respectively), have been studied. The interactions of the complexes with calf thymus-DNA were investigated by UV–vis spectroscopy, CD spectroscopy, and gel electrophoresis. The binding constants of **1** and **2** are 7.2×10^4 and 2.1×10^5 M^{-1}, respectively. The complexes exhibit DNA cleavage activity, with the cleavage process involving oxidative cleavage of DNA.

Keywords: Dinuclear copper coordination polymers; DNA cleavage; Mechanism

1. Introduction

Schiff bases have been widely studied in coordination chemistry [1–3]. Transition metal complexes of Schiff bases have attracted attention due to their remarkable biological

*Corresponding author. Email: zhiqpan@163.com

activities, including antifungal, antibacterial, and antitumor activities [4–6]. Some macrocyclic binuclear transitional metal complexes have been observed to exhibit enhanced DNA binding and cleavage activities [7–10]. These complexes interact with DNA in many modes, such as electrostatic interaction, intercalative binding, and groove binding. A diverse range of factors, including ring size, redox potential, ligand donor strength, and conformational flexibility of macrocyclic complexes, have significant effects on the DNA cleavage abilities of complexes [11, 12]. Our group has synthesized a series of Robson-type Schiff base macrocyclic complexes and studied their magnetic and electrochemical properties, their DNA cleavage properties, and their SOD mimetic activities [13–20]. We recently reported macrocyclic dimers connected by 4,4′-bipyridine moieties [21, 22]. Huang *et al.* reported the self assembly of dinuclear Robson-type macrocyclic complexes, but the properties of the coordination polymers have not yet been studied [23–25].

Although much work has been done on Robson-type macrocyclic complexes incorporating methyl-, chloro-, and bromo-substituents, only a few complexes incorporating fluoro substituents have been reported [21, 26–28]. The fluoro substituent on the phenyl group can influence the properties of Robson-type macrocyclic complexes. As part of ongoing studies on the structures and biological activities of Schiff base complexes, we report the DNA cleavage activity of the 1-D coordination polymers **1** and **2**, which incorporate a 4,4′-bipy bridging the two macrocyclic units. The general structure of the polymers is shown in figure 1. The substituent at the 4-position of the phenyl ring is methyl for **1** and fluoro for **2**. The structures of the polymers have been previously described [29]. The influence of the phenyl substituent on the DNA cleavage activities of the complexes has now been investigated.

2. Experimental

2.1. *Materials and measurements*

All solvents and chemicals were of analytical grade and used as received, except ethanol which was purified to absolute by general method. IR spectra were recorded on a Vector 22 FT-IR spectrophotometer using KBr disks. Elemental analyses were performed on a

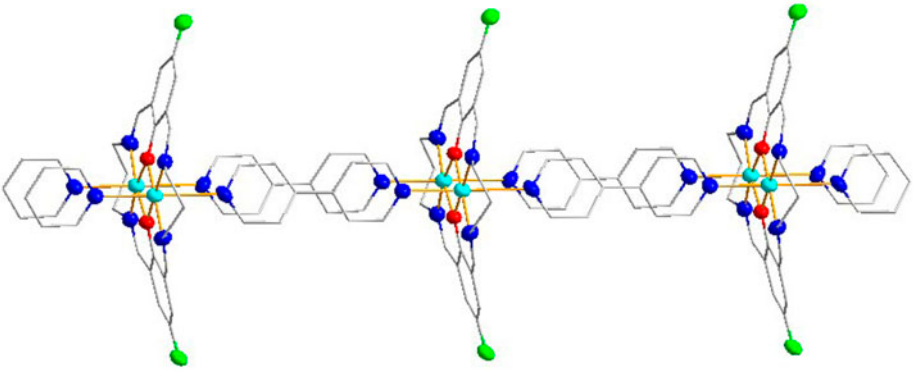

Figure 1. The general structure of the 1-D coordination polymer (the substituent at the 4-position of the phenyl ring is methyl for **1** and fluoro for **2**). Hydrogens have been omitted for clarity (ellipticity 30%).

Perkin-Elmer 240 analyzer. UV–vis spectra were recorded on a Shimadzu UV-2450 spectrophotometer. CD spectra of DNA were obtained using a Jasco J-810 spectropolarimeter.

2.2. *X-ray data collection and refinement*

X-ray structural data were recorded using a Bruker AXS SMART diffractometer (Mo K_α radiation). Data reduction and cell refinement were performed using SMART and SAINT programs [30]. The structures were solved by direct methods (Bruker SHELXTL) and refined on F^2 by full-matrix least squares (Bruker SHELXTL) using all unique data [31]. The non-H atoms in the structure were treated as anisotropic. Hydrogens were located geometrically and refined in riding mode.

2.3. *DNA-binding and cleavage experiments*

Electronic spectra of the complexes were monitored both in the absence and presence of CT DNA. Absorption titration experiments were performed by maintaining the metal complex concentration constant (10 μM) and varying the nucleic acid concentration (0–75 μM). An equal amount of CT DNA was added to both the complex solution and the reference solution to eliminate the absorbance of CT DNA itself. From the absorption titration data, the binding constant was determined using the following equation [32]:

$$[\mathrm{DNA}]/E_{\mathrm{ap}} = [\mathrm{DNA}]/E + 1/(K_{\mathrm{b}}E) \quad (1)$$

$E_{\mathrm{ap}} = \varepsilon_{\mathrm{a}} - \varepsilon_{\mathrm{f}}$, $E = \varepsilon_{\mathrm{b}} - \varepsilon_{\mathrm{f}}$, where ε_{a}, ε_{f}, and ε_{b} correspond to $A_{\mathrm{obsd}}/[\mathrm{Cu}]$, the extinction coefficient for the free complex, and the extinction coefficient for the complex in the fully bound form, respectively. The concentration of CT DNA was determined from its absorption intensity at 260 nm using a molar extinction coefficient of 6600 $\mathrm{M}^{-1}\,\mathrm{cm}^{-1}$ [33]. A plot of $[\mathrm{DNA}]/(\varepsilon_{\mathrm{a}} - \varepsilon_{\mathrm{f}})$ *versus* [DNA] gives the binding constant K_{b} as the ratio of the slope to intercept [34].

The cleavage of plasmid DNA was monitored using agarose gel electrophoresis. The reaction was carried out by mixing 2 μL of PBR322 DNA (0.25 μg $\mu\mathrm{L}^{-1}$) with 4 μL of the complex solution (final concentrations were 12.5, 25, 50, 100, 200, and 400 μM) and diluting with Tris–HCl buffer (pH 7.2) containing 20 mmol NaCl to yield a total volume of 20 μL. The sample was incubated at 37 °C, followed by the addition of the loading buffer containing 0.25% bromphenol blue, 50% glycerol, and 1% Tris, and the solution was finally loaded on 1% agarose gel containing 0.1 μg mL^{-1} ethidium bromide. Electrophoresis was carried out for 1.5 h at 90 V in TAE buffer (40 mmol Tris, 20 mmol acetic acid, 1 mmol EDTA, and pH 7.4). Bands were visualized by UV light and photographed. The solutions for the anaerobic DNA cleavage experiments were prepared in an argon-filled glove box and the reagents incubated for 3 h. All other conditions and procedures were the same as those used for the aerobic experiments. Bands were visualized by UV light and photographed. The intensity of the DNA bands was estimated using a gel documentation system.

3. Results and discussion

3.1. *Preparation of complexes*

3.1.1. $\{[Cu_4L^1(4,4'\text{-bipy})_2](ClO_4)_4\cdot H_2O\}_\infty$ (1). To the mixture of acetonitrile-ethanol (1 : 1, 40 mL) containing 2,6-diformyl-4-methylphenol (0.082 g, 0.5 mmol) and

$Cu(ClO_4)_2 \cdot 6H_2O$ (0.186 g, 0.5 mmol), four drops of triethylamine was added. Then 1,3-diaminopropane (0.037 g, 0.5 mmol) in acetonitrile-ethanol (1 : 1, 10 mL) was slowly added. The mixture was stirred for 4 h, then 4,4′-bipy (0.312 g, 2 mmol) in acetonitrile-ethanol (1 : 1, 10 mL) was introduced. The mixture was refluxed for 1 h, then cooled to room temperature and filtered. Green crystals of 1 were obtained by vapor diffusion of diethyl ether into solution of the complex in acetonitrile–ethanol. Yield: 0.26 g, 63%. Anal. Calcd for $C_{34}H_{34}Cu_2Cl_2N_6O_{13}$: C, 43.78; H, 3.67; N, 9.01. Found: C, 44.58; H, 3.37; N, 8.73. IR (KBr, ν/cm^{-1}): 1638($\nu_{C=N}$), 1101(ν_{ClO4}^{-}), 639 (δ_{ClO4}^{-}).

3.1.2. $\{[Cu_4L^2(4,4'\text{-bipy})_4](ClO_4)_4 \cdot 2CH_3CN \cdot 2H_2O\}_\infty$ (2). Complex 2 was obtained using the same procedure as used for **1**, except that 2,6-diformyl-4-fluorophenol was used. Yield: 0.136 g, 29%. Anal. Calcd for $C_{88}H_{82}Cl_4Cu_4F_4N_{18}O_{22}$: C, 47.70; H, 3.73; N, 11.38. Found: C, 44.62; H, 3.79; N, 11.43. IR (KBr, ν/cm^{-1}): 3055, 2918 (C–H), 1638 ($\nu_{C=N}$), 1079 (ν_{ClO4}^{-}), 631 (δ_{ClO4}^{-}).

3.2. *Absorption spectroscopic studies*

UV–vis spectroscopy was used to monitor the interaction of 1 and **2** with CT DNA. Typically a complex incorporating an aromatic ligand intercalates with DNA leading to hypochromism and a red shift of the absorption band(s) due to a strong π stacking interaction between the aromatic ligand of the complex and the DNA base pairs [35–39]. As shown in figures 2 and 3, bands centered at ~370 nm exhibit hypochromism accompanied by a red shift for both complexes. With increasing CT-DNA concentration for **1**, the decrease in intensity of the 362 nm band is 54%, with a red shift of 3.2 nm at a ratio of [DNA]/[Cu] of 7.5. The band at 358 nm in **2** decreases by 36%, and a red shift of 4.5 nm occurs under the same experimental conditions. These spectral characteristics suggest that the complexes interact with DNA via π stacking of the aromatic ligand of the complex with

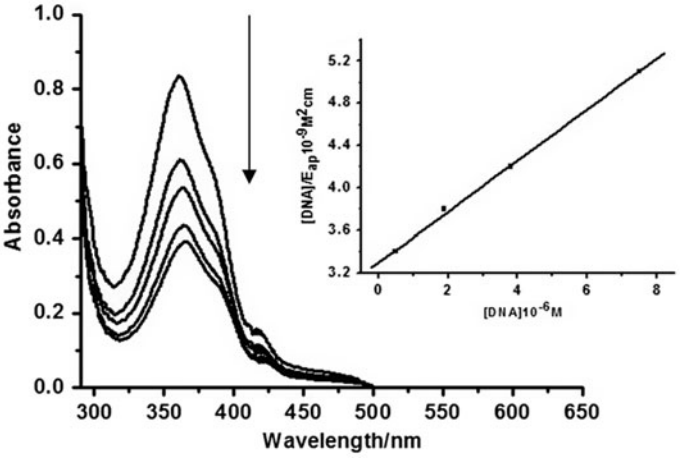

Figure 2. Absorption spectra of **1** (10 μM) in Tris–HCl buffer upon addition of calf thymus DNA (0–75 μM). The arrow shows the decrease in absorbance with increasing DNA concentration. Inset: Plots of $[DNA]/(\varepsilon_a - \varepsilon_f)$ *versus* [DNA] for CT-DNA with **1**.

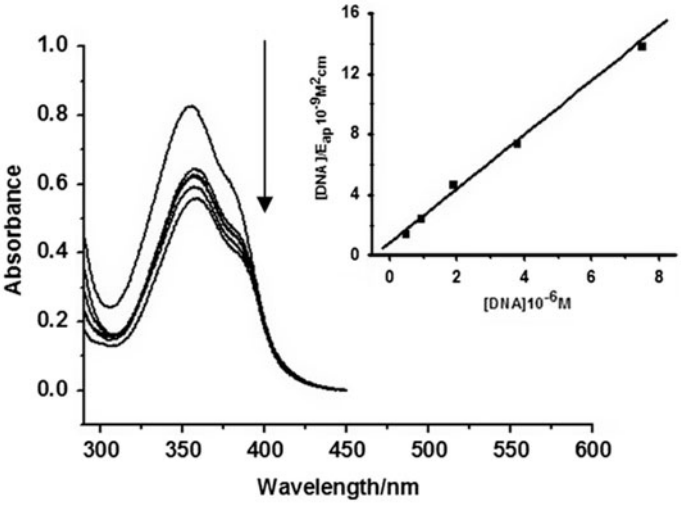

Figure 3. Absorption spectra of **2** (10 μM) in Tris–HCl buffer upon addition of calf thymus DNA(0–75 μM). The arrow shows the decrease in absorbance with increasing DNA concentration. Inset: Plots of [DNA]/($\varepsilon_a - \varepsilon_f$) *versus* [DNA] for CT-DNA with **2**.

the base pairs of DNA [40]. To compare the binding strength of the complexes with CT DNA, the intrinsic binding constants K_b were determined using equation (1). A plot of [DNA]/($\varepsilon_a - \varepsilon_f$) *versus* [DNA] gave K_b values of 7.2 (±0.04) × 10^4 M^{-1} for **1** and 2.1 (±0.07) × 10^5 M^{-1} for **2**, respectively. The K_b values are much smaller than those reported for the classical intercalator ethidium bromide (~10^6 M^{-1}) [41], but are similar to those reported for $[Cu_4(oxbe)_2(bpy)_2](ClO_4)_2{\cdot}2H_2O$ ($K_b = 1.47 \times 10^5$ M^{-1}) [42], $[Cu_2(heap)(H_2O)_2](pic)_2{\cdot}2H_2O$ ($K_b = 2.67 \times 10^4$ M^{-1}) [43]), $[Cu_2L(phen)(H_2O)_3(ClO_4)](ClO_4)_3$ ($K_b = 3.02 \times 10^5$ M^{-1}) [44], and $[Cu_2L(H_2O)_2](phen)_2(ClO_4)_2$ [45], and larger than those reported for $[Cu_2L_2(H_2O)]_\infty$ ($K_b = 4.91 \times 10^3$ M^{-1}), $\{[Cu_2L_2(H_2O)]{\cdot}H_2O\}_\infty$ ($K_b = 8.75 \times 10^3$ M^{-1}) [46].

3.3. *CD spectroscopy studies*

Figure 4 shows CD spectra for CT DNA treated with **1** and **2** with the ratio of 0.4 : 1 complex: DNA. Both the positive (~275 nm) and negative (~245 nm) bands decreased in intensity with the addition of the complex, which is a clear indication that non-classical intercalation occurs between the complex and DNA. This suggests that the complexes can unwind the DNA helix leading to a loss of helicity [47]. The largest decrease in the CD band intensity was observed for **2**, suggesting that **2** is more effective than **1** in perturbing the secondary structure of DNA at the same concentration. From the results of CD spectroscopy studies, one can conclude that **2** binds to CT DNA more effectively than **1**, which is consistent with the UV–vis spectroscopy results.

The spectroscopic results provide support for the phenyl rings playing an important role in DNA cleavage, given that **1** and **2** differ only in the phenyl ring substituent (methyl for **1** and fluoro for **2**). The spatial requirement of fluorine is less than that of methyl, so the former may enhance the π stacking interaction between the aromatic ring of the complex

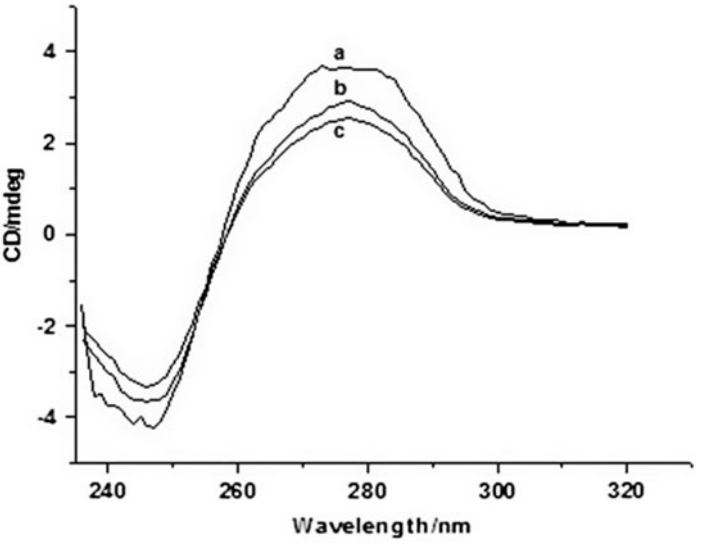

Figure 4. CD spectra of CT DNA (1.0×10^{-4} M) in the absence (a) and presence of **1** (b) and **2** (c) with a [complex] : [DNA] ratio of 0.4 : 1.

and the DNA base pairs. This result is in agreement with previous results from our group [20, 48].

3.4. *Interaction between the complexes and plasmid DNA (pBR 322)*

The DNA cleaving ability of **1** and **2** has been investigated for a range of complex concentrations at various incubation times. Figures 5–7 show the results of gel electrophoresis experiments carried out with supercoiled DNA in the absence and presence of **1** and **2**. Lane 1 in the figures shows a DNA control in the absence of either complex. In the absence of the complex, DNA remains in the supercoiled form, while incubation of DNA with the complex leads to conversion from form I to form II. The amount of form II formed is dependent on the concentration of complexes; however, increasing the incubation time has no effect on the cleavage activity. Upon increasing the concentration of the complexes, the intensity of the circular supercoiled DNA band decreases, while that of the nicked band increases. Data quantifying the percentage of plasmid relaxation (the % of form II) relative to plasmid DNA per lane is given in the supplementary material (figure S1 [see online supplemental material at http://dx.doi.org/10.1080/00958972.2015.1032272] for **1** and figure S2 for **2**, respectively). The mechanism of cleavage has been probed using different reagents. For **1**, the addition of NaN_3 does not inhibit cleavage (57% Form II), suggesting that the reactive oxygen species (ROS) singlet oxygen is not responsible for cleavage [49]. Addition of KI and DMSO, however, inhibit DNA cleavage (31 and 29% form II, respectively). This suggests a mechanistic pathway involving formation of $^{\cdot}OH$ and H_2O_2 [50]. For **2**, addition of DMSO shows a significant reduction in cleavage (no observable form II), suggesting that $^{\cdot}OH$ is the ROS responsible for DNA cleavage [51]. As shown in figure 7, there is no DNA cleavage activity for **1** and **2** under anaerobic conditions. This implies that DNA cleavage by **1** and **2** occurs via oxidation.

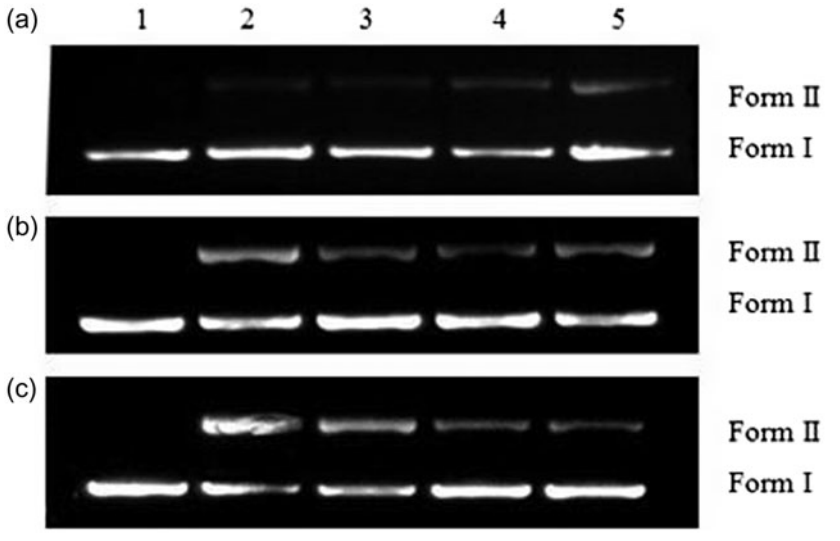

Figure 5. Electrophoresis gels showing cleavage of pBR322 DNA (0.25 μg μL^{-1}) by **1** at varying conditions in 50 mmol Tris–HCl/NaCl buffer (pH 7.2) at 37 °C. (a) Lane 1, DNA control; Lanes 2–5, DNA + **1** (25, 50, 100, and 200 μM), respectively; (b) Lane 1, DNA control; Lanes 2–5, DNA + **1** (100 μM) for 1, 2, 3, and 4 h; (c) Lane 1, DNA control; Lane 2, DNA + **1** (200 μM); Lanes 3–5, DNA + **1** (200 μM) + 5 mmol NaN_3, KI, or DMSO.

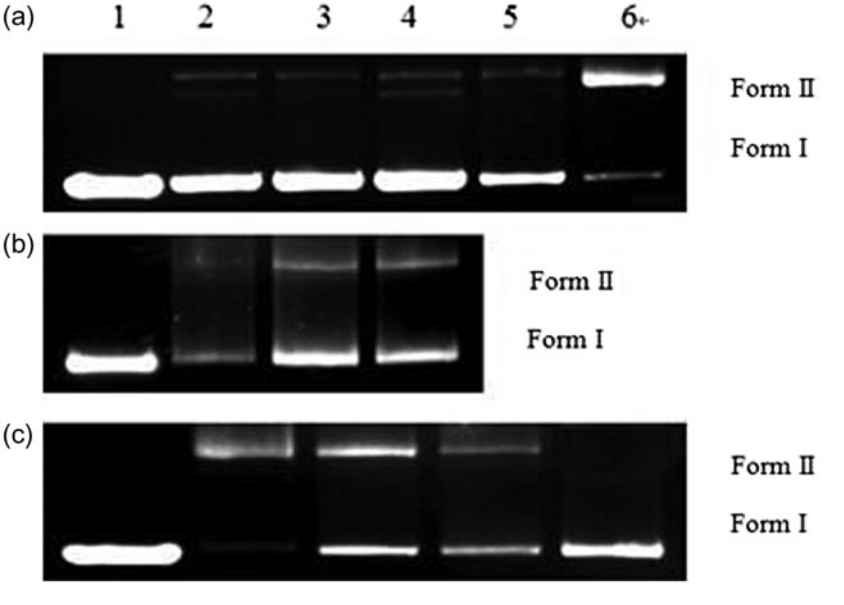

Figure 6. Electrophoresis gels showing cleavage of pBR322 DNA (0.25 μg μL^{-1}) by **2** at varying conditions in 50 mmol Tris–HCl/NaCl buffer (pH 7.2) at 37 °C. (a) Lane 1, DNA control; Lanes 2–5, DNA + **2** (25, 50, 100, and 200 μM), respectively; (b) Lane 1, DNA control; Lanes 2–4, DNA + **2** (100 μM) for 1, 2, and 3 h; (c) Lane 1, DNA control; Lane 2, DNA + **2** (200 μM); Lanes 3–5, DNA + **2** (200 μM) + 5 mmol NaN_3, KI, or DMSO.

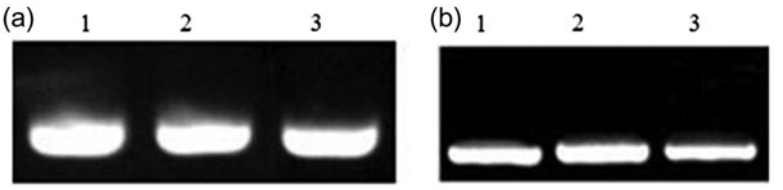

Figure 7. pBR322 DNA (0.25 μg μL^{-1}) incubated for 3 h in the presence of complexes under anaerobic conditions at pH 7.2 and 20 °C. (a) Lane 1, DNA control; Lanes 2 and 3, DNA + **1** (100 and 200 μM); (b) Lane 1, DNA control; Lanes 2 and 3, DNA + **2** (100 and 200 μM).

4. Conclusion

Two 1-D macrocyclic dinuclear coordination polymers featuring 4,4′-bipy bridging the two macrocyclic units were prepared and structurally characterized. UV–vis and CD spectroscopy experiments showed that the complexes bind DNA in a non-classical intercalative mode. The DNA cleavage activity of the complex is dependent on the phenyl substituent (CH_3 or F) of the macrocyclic ligand. The complex incorporating a fluoro substituent has increased DNA cleavage activity compared with the complex with the methyl substituent. The mechanism for DNA cleavage by **1** and **2** involves oxidation.

Supplementary material

CCDC 837666 and CCDC 837665 contain the supplementary crystallographic data for **1** and **2**. These data can be obtained free of charge via http://www.ccdc.cam.ac.uk/conts/retrieving.html, or from the Cambridge Crystallographic Data Center, 12 Union Road, Cambridge CB2 1EZ, UK; Fax: (+44) 1223-336-033; or E-mail: deposit@ccdc.cam.ac.uk.

Disclosure statement

No potential conflict of interest was reported by the authors.

Funding

This work was financial support from the National Nature Science Foundation of China [grant number 21301131], [grant number 21477118]; the Nature Science Foundation of Hubei Province [grant number 2013 CFB313]; the open fund of the Engineering Research Center of Nano-Geo Materials of the Ministry of Education China University of Geosciences, Wuhan, the scientific research fund of the Wuhan Institute of Technology [grant number K201471]; the Key Program of the Natural Science Foundation of Hubei Province [grant number 2014CFA530]; the Foundation of the Key Laboratory for Green Chemical Process of Ministry of Education, Wuhan Institute of Technology [grant number RGCT200804].

References

[1] Q.R. Cheng, H. Zhou, Z.Q. Pan, J.Z. Chen. *Transition Met. Chem.*, **37**, 407 (2012).
[2] C. Adhikary, R. Sen, G. Bocelli, A. Cantoni, M. Solzi, S. Chaudhuri. *J. Coord. Chem.*, **62**, 3573 (2009).

[3] C.X. Zhang, C.X. Cui, M. Lu, L. Yu, Y.X. Zhan. *Synth. React. Inorg. Met.-Org. Nano-Met. Chem.*, **39**, 136 (2009).
[4] Z.C. Liu, B.D. Wang, Z.Y. Yang, Y. Li, D.D. Qin, T.R. Li. *Eur. J. Med. Chem.*, **44**, 4477 (2009).
[5] D.D. Qin, Z.Y. Yang, G.F. Qi, T.R. Li. *Transition Met. Chem.*, **34**, 499 (2009).
[6] Y.Y. Yu, H.D. Xian, J.F. Liu, G.L. Zhao. *Molecules*, **14**, 1747 (2009).
[7] A. Arbuse, M. Font, M.A. Martínez, X. Fontrodona. *Inorg. Chem.*, **48**, 11098 (2009).
[8] S. Anbu, M. Kandaswamy, P. Suthakaran, V. Murugan, B. Varghese. *J. Inorg. Biochem.*, **103**, 401 (2009).
[9] Y. He, X.H. Wang, H. Zhou, Z.Q. Pan, J.B. Li, Q.M. Huang. *Inorg. Chem. Commun.*, **13**, 314 (2010).
[10] Y.F. Chen, L. Wei, J.L. Bai, H. Zhou, Q.M. Huang, J.B. Li, Z.Q. Pan. *J. Coord. Chem.*, **64**, 1153 (2011).
[11] J.G. Muller, X. Chen, A.C. Dadiz, S.E. Rokita, C.J. Burrows. *J. Am. Chem. Soc.*, **114**, 6407 (1992).
[12] Y. Zhao, J. Zhu, W. He, Z. Yang, Y. Zhu, Y. Li, J. Zhang. *Chem. Eur. J.*, **12**, 6621 (2006).
[13] B. Liu, H. Zhou, Z.Q. Pan. *Transition Met. Chem.*, **30**, 1020 (2005).
[14] Q.M. Huang, S.R. Li, Z.H. Peng, H. Zhou. *Inorg. Chem. Commun.*, **13**, 867 (2010).
[15] J. Pan, L. Cheng, H. Zhou. *Polyhedron*, **29**, 1588 (2010).
[16] H. Zhou, Z.H. Peng, Z.Q. Pan. *Polyhedron*, **26**, 3233 (2007).
[17] H. Zhou, Z.H. Peng, Z.Q. Pan. *J. Coord. Chem.*, **58**, 443 (2005).
[18] H. Zhou, Z.H. Peng, Z.Q. Pan. *J. Mol. Struct.*, **743**, 59 (2005).
[19] L. Chen, J.L. Bai, H. Zhou. *J. Coord. Chem.*, **61**, 1412 (2008).
[20] Q.R. Cheng, J.Z. Chen, H. Zhou. *J. Coord. Chem.*, **64**, 1139 (2011).
[21] Q.R. Cheng, H. Zhou, Z.Q. Pan, J.Z. Chen. *Polyhedron*, **30**, 1171 (2011).
[22] Q.R. Cheng, Z.Q. Pan, H. Zhou, J.Z. Chen. *Inorg. Chem. Commun.*, **14**, 929 (2011).
[23] W. Huang, S.H. Gou, D.H. Hu. *Inorg. Chem.*, **40**, 1712 (2001).
[24] W. Huang, S.H. Gou, D.H. Hu. *Inorg. Chem.*, **41**, 864 (2002).
[25] W. Huang, H.B. Zhu, S.H. Gou. *Coord. Chem. Rev.*, **250**, 414 (2006).
[26] L. Chen, J.L. Bai, H. Zhou, Z.Q. Pan, Q.M. Huang, Y. Song. *J. Coord. Chem.*, **61**, 1412 (2008).
[27] J.L. Bai, H. Zhou, Z.Q. Pan. *Chin. J. Inorg. Chem.*, **24**, 1994 (2008).
[28] J.L. Bai, H. Zhou, Z.Q. Pan. *Acta Crystallogr.*, **E63m2641**, Sm2641/1 (2007).
[29] Q.R. Cheng, H. Zhou, Z.Q. Pan. *Polyhedron*, **81**, 668 (2014).
[30] Smart and Saint. *Area Detector Control and Integration Software*, Siemens Analytical X-Ray Systems Inc., Madison, Wisconsin, USA (1996).
[31] G.M. Sheldrick, *SHELXTL V5.1 Software Reference Manual*, Bruker AXS, Inc., Madison, Wisconsin, USA (1997).
[32] V. Uma, M. Kanthimathi, J. Subramanian. *Biochim. Biophys. Acta*, **1760**, 814 (2006).
[33] A. Wolfe, G.H. Shimer, T. Meehan. *Biochemistry*, **26**, 6392 (1987).
[34] C.W. Jiang, H. Chao, X.L. Hong. *Inorg. Chem. Commun.*, **6**, 773 (2003).
[35] H. Li, X.Y. Le, D.W. Pang. *J. Inorg. Biochem.*, **99**, 2240 (2005).
[36] J.K. Barton, A.T. Danishefsky, J.M. Goldberg. *J. Am. Chem. Soc.*, **106**, 2172 (1984).
[37] T.M. Kelly, A.B. Tossi, D.J. McConnel, T.C. Strekas. *Nucleic Acids Res.*, **13**, 6017 (1985).
[38] A. Tysoe, R.J. Morgan, A.D. Baker, T.C. Strekas. *J. Phys. Chem.*, **97**, 1707 (1993).
[39] N. Raman, A. Sakthivel, R. Jeyamurugan. *J. Coord. Chem.*, **62**, 3969 (2009).
[40] F. Gao, H. Chao, F. Zhou, Y.X. Yuan, B. Peng, L.N. Ji. *J. Inorg. Biochem.*, **100**, 1487 (2006).
[41] J.B. LePecq, C. Paoletti. *J. Mol. Biol.*, **27**, 87 (1967).
[42] X.W. Li, M. Jiang, Y.T. Li, Z.Y. Wu, C.W. Yan. *J. Coord. Chem.*, **63**, 1582 (2010).
[43] X.W. Zhang, Y.J. Zheng, Y.T. Li, Z.Y. Wu, C.W. Yan. *J. Coord. Chem.*, **63**, 2985 (2010).
[44] S. Anbu, A. Killivalavan, E.C.B.A. Alegria, G. Mathan, M. Kandaswamy. *J. Coord. Chem.*, **66**, 3989 (2013).
[45] J. Lu, J.L. Li, Q. Sun, L. Jiang. *J. Coord. Chem.*, **67**, 300 (2014).
[46] C. Gao, X. Ma, J. Lu, Z. Wang, J. Tian, S. Yan. *J. Coord. Chem.*, **64**, 2157 (2011).
[47] K. Karidi, A. Garoufis, N. Hadjiliadis, J. Reedijk. *Dalton Trans.*, **4**, 728 (2005).
[48] Z.Q. Pan, K. Ding, H. Zhou, Q.R. Cheng. *Polyhedron*, **30**, 2268 (2011).
[49] K. Dhara, P. Roy, J. Ratha. *Polyhedron*, **26**, 4509 (2007).
[50] Y. Shao, X. Sheng, Y. Li. *Bioconjugate Chem.*, **19**, 1840 (2008).
[51] Y.M. Zhao, J.H. Zhu, W.J. He. *Chem. Eur. J.*, **12**, 6621 (2006).